International Journal of Engineering & Technology, 7 (2) (2018) 759-763

International Journal of Engineering & Technology

Website: www.sciencepubco.com/index.php/IJET
doi: 10.14419/ijet.v7i2.11139
Research paper

Parametric resonance of shaft with variable slenderness ratio

N. Omar [1], A. M. A. Wahab [1], Z. A. Rasid [1] *, A. Abu [1], N. F. M. N. Rudin [1]

[1] IDS i-Kohza Malaysia-Japan International Institute of Technology Universiti Teknologi Malaysia 54100 UTM Kuala Lumpur Malaysia
**Corresponding author E-mail: arzainudin.kl@utm.my*

Abstract

Parametric instability of a shaft occurs within a certain range of speed when the shaft parameters such as stiffness and mass are disturbed periodically. At high speed a shaft may carry high torque and as such the effect of torsion on the parametric instability need to be considered. The use of the Timoshenko's beam theory in the parametric instability formulation of shaft in the past has seen this torsional effect being neglected. In this paper the torsional degree of freedom is added to the formulation for the parametric instability of shaft that is based on the mentioned Timoshenko's theory. The focus is on the effect of slenderness ratio of shaft on the occurrence of parametric instability on the shaft. The finite element method is used to produce the Mathieu-Hill equation and upon applying the Bolotin's method the parametric insta-bility equations of shaft can be determined. The formulation and its corresponding MATLAB source codes were successfully validated based on past results. It was found that the increase in the slenderness ratio has shifted the instability chart to the right by 20 %. Furthermore the additional torsional degree of freedom has significantly changed the instability chart of the shaft at high speed.

Keywords: *The Bolotin's Method; Instability Chart; The Mathieu-Hill Equation: Parametric Instability; The Timoshenko's Beam Theory.*

1. Introduction

The unstable condition due to excessive vibration in a shaft system can contribute to noise, uncomfortable feeling to the machine users and eventually may lead to failure to the system. Two sources of instability are force resonance and parametric resonance or instability. While force resonance is known to occur when input frequency is equal to natural frequency of rotor system, parametric instability occurs when a shaft experiencing periodic change in its parameter rotates within a certain range of speed. As this parametric instability happens the shaft vibrates unboundedly and this may damage the equipment if it occurs continuously. In parametric instability analysis the instability chart or the so called the Strut-Ince diagram such as shown in Figure 1 [1] is sought to give the stable and unstable operating regions of the shaft for several modes of instability.

Finite element method (FEM) has been used greatly in modelling the parametric instability behavior of shaft [2-4]. Beam theories have been applied to represent shaft as the effects of the lateral displacement, transverse shear displacement and gyroscopic are included in the formulation. The Euler-Bernoulli beam theory is commonly used especially in slender beam condition due to its simplicity and reasonable approximation [5]. However without considering the transverse shear displacement and the gyroscopic effect, the approximation of the natural frequency tends to be inaccurate especially at higher mode. The Rayleigh's beam theory enhanced the Euler-Bernoulli's beam theory by adding the effect of rotation of the cross section of the beam [6]. The better beam theory is the Timoshenko's beam theory [7-8] because it considers all the stated effects which allow the theory to be applied in slender or non-slender shaft. However at present, in industries such as aircraft and automotive, operating rotor system at high speed has becoming a practice to increase the efficiency of the equipment [9]. At high speed the shaft may carry high torque such that the torsional effect on the shaft should be considered in the formulation but this has been neglected in the past. The work of Nelson and co-workers [10-12] considered the torsional degree of freedom in their shaft instability study and they found that the accuracy of the results has improved with the number of finite elements used. But their work was limited to the whirling frequency and unbalanced response analysis of a rotor system.

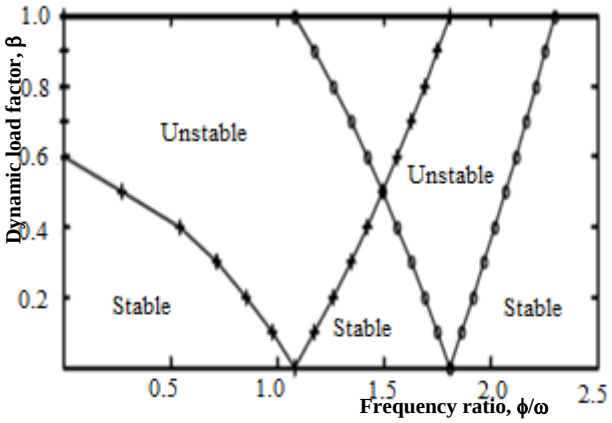


Fig. 1: The Instability Chart [1]: β = Dynamic Load Factor, ϕ = Frequency of the Axial Excitation, ω = Natural Frequency of the Rotor System.

In this study finite element method (FEM) was used to model the parametric instability behavior of high speed rotating shaft while considering the effect of the torsional motion. The Mathieu-Hill equation that represents the parametric instability behavior of shaft was developed. Upon applying the Bolotin's method [13], the equation for the parametric instability problem of shaft that can give the instability chart can be determined. The formulation has been coded in MATLAB's environment and validated using past

Copyright © 2018 N. Omar et al. This is an open access article distributed under the Creative Commons Attribution License, which permits unrestricted use, distribution, and reproduction in any medium, provided the original work is properly cited.

results. In this paper the focus is on the effect of the slenderness ratio of the shaft on the parametric instability of the shaft system. A comparison is made between the results correspond to the commonly used Timoshenko's beam theory formulation that requires four degree of freedom to the results correspond to the formulation that includes the torsional degree of freedom.

2. Material and method

A simple shaft supported with rigid bearings at its both ends such as shown in Figure 2 is studied here. P(t) is the periodically changed axial load that causes the periodic change in the stiffness of the shaft.

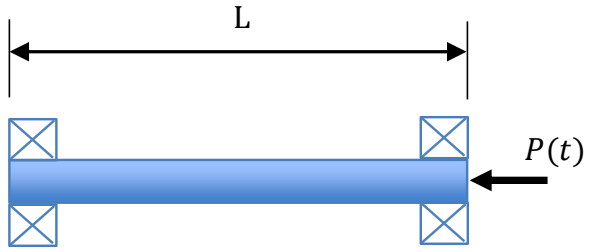


Fig. 2: The Shaft Understudy: L = Length of Shaft, P (T) = Periodic Axial Load.

The geometry and material properties of the shaft are given in Table 1. The radius of the shaft, r can be calculated from the applied slenderness ratio, r_s = L/r where L is the length of the shaft.

Table 1: Geometry and Material Properties of the Shaft

Item	Value
Young's modulus, E	207 GPa
Modulus of rigidity, G	79.6 GPa
Poisson's ratio, v	0.303
Density, ρ	7833 kg/m^3
Length, L	1.27 m
Shear factor, κ	0.9

The finite element formulation developed here is based on the Timoshenko's beam theory while applying the Nelson's FEM approach [10] that considers the torsional effect of the shaft. Referring to Figure 3 the beam element has 2 nodes per element. Each node considers 5 degrees of freedom (dof): v, w, θ_y, θ_z and θ_x. v and w are the translations in y and z directions respectively θ_y and θ_z are the rotations about y and z axis respectively and the additional dof θx is the rotation about x axis. The results correspond to this so called the 5DOF model is compared to the results correspond to the typical Timoshenko's beam that omits the torsional dof θ_x. The later model in this paper is called the 4DOF model.

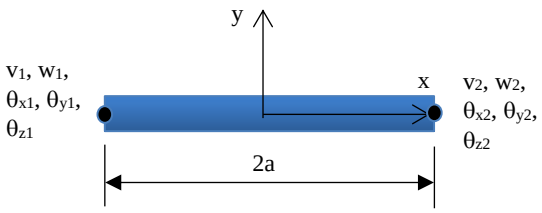


Fig. 3: The Beam Element: 2a = Length of Shaft.

The strains due to bending load are

$$\varepsilon_{y_b} = \frac{\partial v}{\partial x} = -y\frac{\partial \theta_z}{\partial x}$$

$$\varepsilon_{z_b} = \frac{\partial w}{\partial x} = z\frac{\partial \theta_y}{\partial x}$$

$$\varepsilon_{x_b} = \frac{\partial u}{\partial x} = 0 \qquad (1)$$

$$\varepsilon_{xy_b} = \frac{\partial u}{\partial y} + \frac{\partial v}{\partial x} = -\theta_z(x) + \frac{\partial v(x)}{\partial x}$$

$$\varepsilon_{xz_b} = \frac{\partial u}{\partial z} + \frac{\partial w}{\partial x} = \theta_y(x) + \frac{\partial w(x)}{\partial x}$$

While the strains due to torsional load are

$$\varepsilon_{x_t} = \frac{\partial^2 \theta_x}{\partial x^2}\psi$$

$$\varepsilon_{xy_t} = \frac{\partial u}{\partial y} + \frac{\partial v}{\partial x} = \frac{\partial \theta_x}{\partial x}\left(\frac{\partial \psi}{\partial y} - z\right) \qquad (2)$$

$$\varepsilon_{xz_t} = \frac{\partial u}{\partial z} + \frac{\partial w}{\partial x} = \frac{\partial \theta_x}{\partial x}\left(\frac{\partial \psi}{\partial y} + y\right)$$

Considering the bending, transverse shear, torsional and the external load P, the potential energy of the shaft U is

$$U = \frac{1}{2}\int_{-a}^{+a} EI_p\left(\left(\frac{d\theta}{dz}\right)^2 + \left(\frac{d\theta}{dy}\right)^2\right) dx +$$

$$\frac{1}{2}\int_{-a}^{+a} \kappa GA\left(\frac{dv}{dx} - \theta_z\right)^2 + \kappa GA\left(\frac{dw}{dx} + \frac{d\theta}{dy}\right)^2 dx +$$

$$\frac{1}{2}\int_{-a}^{+a} GJ\left(\frac{d\theta}{dx}\right)^2 dx - \frac{1}{2}\int_{-a}^{+a} P\left[\left(\frac{dv}{dx}\right)^2 + \left(\frac{dw}{dx}\right)^2\right]dx \qquad (3)$$

Where E and G are the Young's modulus and the shear modulus of the shaft respectively. I_p is the total second moment of inertia, J is the polar moment of inertia and A is the cross-sectional area of the shaft. k is the shear correction factor and P is the axial force. Notice that the third term of equation (3) gives the potential energy corresponds to the additional torsional dof. Following this the formulation for kinetic energy T of the rotating shaft is

$$T = \frac{1}{2}\int_{-a}^{+a} \rho A\left(\left(\frac{\partial v}{\partial t}\right)^2 + \left(\frac{\partial w}{\partial t}\right)^2\right) dx$$

$$+ \frac{1}{2}\int_{-a}^{+a} \rho I_y\left(\frac{\partial \theta_y}{\partial t}\right)^2 + \rho I_z\left(\frac{\partial \theta_z}{\partial t}\right)^2 dx + \frac{1}{2}\int_{-a}^{+a} \rho I_x \theta_z \frac{\partial \theta_y}{\partial t}\Omega\, dx$$

$$+ \frac{1}{2}\int_{-a}^{+a} \rho I_x \theta_z\left(\frac{\partial \theta_x}{\partial t}\right)^2 dx \qquad (4)$$

Where ρ and Ω are the density and the spin speed of the shaft respectively. I_x, I_y and I_z are the moment of inertia with respect to x, y and z axis respectively.
Following the standard FEM procedures of discretization of the shaft and upon assembly process of elemental matrices, the potential energy, U and kinetic energy, T of rotating Timoshenko shaft subjected to periodic axial loading can be stated in terms of global displacement vector {q} such as shown below.

$$U = \frac{1}{2}\{q\}^T[K]\{q\} - \frac{1}{2}\{q\}^T P(t)\left[K_g\right]\{q\} \qquad (5)$$

$$T = \frac{1}{2}\{\dot{q}\}^T[M]\{\dot{q}\} + \frac{1}{2}\{\dot{q}\}^T\Omega[G]\{q\} \qquad (6)$$

Where the matrices [K], [M], [G] and $\left[K_g\right]$ are the global elastic stiffness matrix, global mass matrix, global gyroscopic matrix and global geometric stiffness matrix respectively of the shaft system. Applying the Lagrange's equation, the governing equation is

$$[M]\{\ddot{q}\} + \Omega[G]\{\dot{q}\} + ([K] - P(t)\left[K_g\right])\{q\} = 0 \qquad (7)$$

And representing the periodic axial force as

$$P(t) = \alpha P^* + \beta P^* \cos \phi t \qquad (8)$$

Where α and β as static and dynamic load factors respectively, we have the standard FEM governing equation that represents periodic loading of a shaft such as

$$[\mathrm{M}]\{\ddot{\mathrm{q}}\} + \Omega[\mathrm{G}]\{\dot{\mathrm{q}}\} + ([\mathrm{K}] - [\mathrm{K_g}](\alpha \mathrm{P}^* + \beta \mathrm{P}^* \cos \phi \mathrm{t}\,(\mathrm{t}))\{\mathrm{q}\} = 0 \quad (9)$$

Equation (9) represents the second order differential equations with periodic coefficients of the Mathieu-Hill equation type. Applying the Bolotin's method, an equation that represents the parametric instability problem of shaft to be solved in this study can be written such as:

$$\left[\begin{bmatrix} [K] + \left(\alpha - \frac{\beta}{2}\right)[K_g] & 0 \\ 0 & [K] + \left(\alpha + \frac{\beta}{2}\right)[K_g] \end{bmatrix} + \phi \begin{bmatrix} 0 & -\frac{1}{2}\Omega[G] \\ \frac{1}{2}\Omega[G] & 0 \end{bmatrix} + \phi^2 \begin{bmatrix} -\frac{1}{4}[M] & 0 \\ 0 & -\frac{1}{4}[M] \end{bmatrix}\right] = 0 \quad (10)$$

Equation (10) is a quadratic eigen-value problem that can give the lower and upper boundary curves of the principal instability region.

3. Results and discussion

This section starts with the validation of the developed formulation and the MATLAB's codes followed by the results of the parametric studies conducted focusing on the effect of the slenderness ratio of the shaft.

3.1. Validation

Dynamic instability analysis was conducted on static and rotating simply supported shafts subjected to periodic axial compressive load. The results are compared to the work of Chen and Ku [14] that used Timoshenko beam element which applied 4 degrees of freedom per node in their study. Figure 4 shows the plots of the dynamic load factor β against the frequency ratio that represents the parametric instability regions for the shafts where the regions in between the V-shape lines represent the unstable region (US) as indicated in the diagram.
For the stable regions (S), the system will go toward stable equilibrium position as disturbance occurs. Figure 4 also shows that the instability regions obtained in the current works are in great agreement with those of the past researchers [14].

3.2. The effect of the slenderness ratio

Figure 5-7 show the parametric instability of shafts having different slenderness ratios correspond to the 4DOF and 5DOF models for shafts having simply supported boundary condition. At static condition as in Figure 5, the 1st and 2nd modes of instability region do not change as slenderness ratio varies for both 4DOF and 5DOF models. However for the 3rd mode of instability region, the region shifts to lower value as the slenderness ratio is increased. This result is in line with the work of Sabuncu and Evran [15]. As rotating speed increases to 9000 RPM the parametric instability regions for the 5DOF model are enlarged equally for both low and high slenderness ratios as shown in Figure 6.

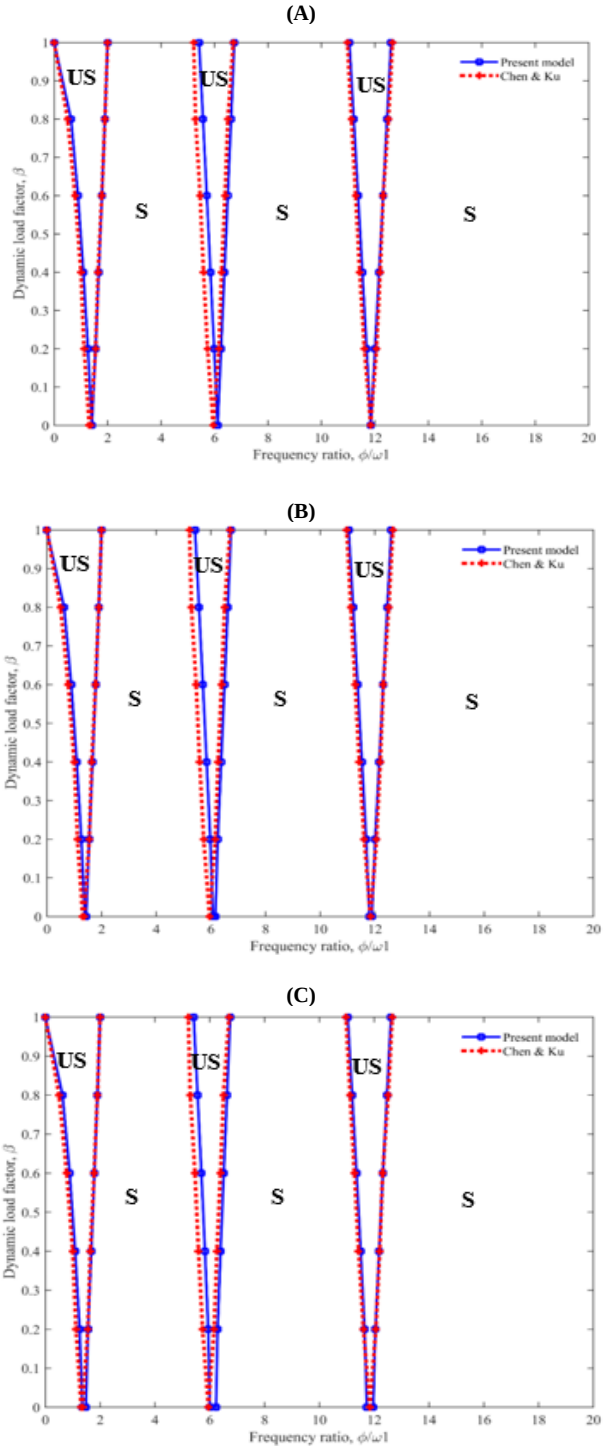


Fig. 4: The Validation of the Dynamic Instability Charts for Simply Supported Shaft at: (A) 0 RPM (B) 8000 RPM (C) 20000 RPM: S = Stable Region, US = Unstable Region.

For the 4DOF model, the region of parametric instability is larger at higher mode for shaft with high slenderness ratio compared to shaft with lower one. It shows that at the higher mode, the shaft with lower slenderness ratio is more stable compared to the shaft having higher slenderness ratio.
The parametric instability region enlarges again as rotating speed increases to 40000 RPM such as shown in Figure 7. For the 4DOF model, the parametric instability region is larger for high slenderness ratio compared to that of the lower slenderness ratio. It can be said that the shaft system with larger diameter is more unstable compared to that of smaller diameter. In contrast, the parametric instability region is smaller as high slenderness ratio is applied to shaft, applying the 5DOF model. In this case larger diameter of shaft is more stable compared to smaller one. This difference in results shows the significant effect of torsional motion that is con-

sidered in the 5DOF model for the case changing the slenderness ratio of the shaft.

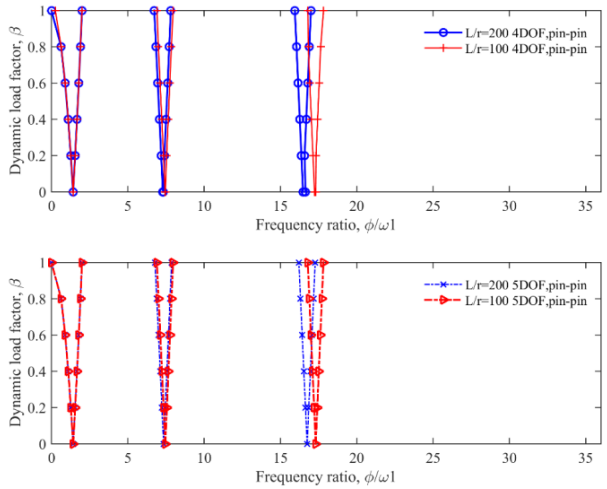


Fig. 5: The Effect of the Slenderness Ratio on the Parametric Instability of Shaft at 0 RPM: L/R = Slenderness Ratio.

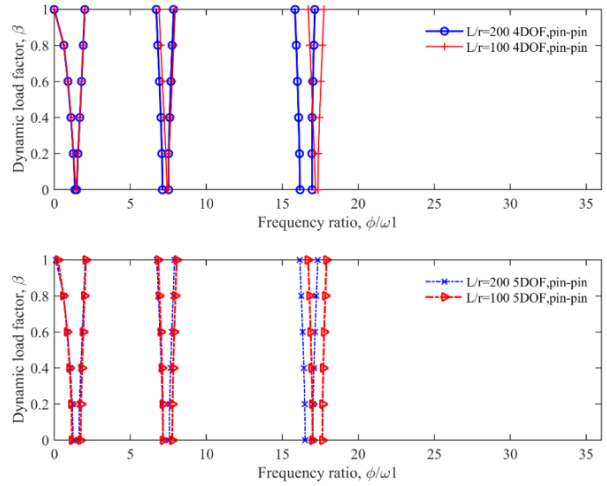


Fig. 6: The Effect of the Slenderness Ratio on the Parametric Instability of Shaft at 0 RPM.

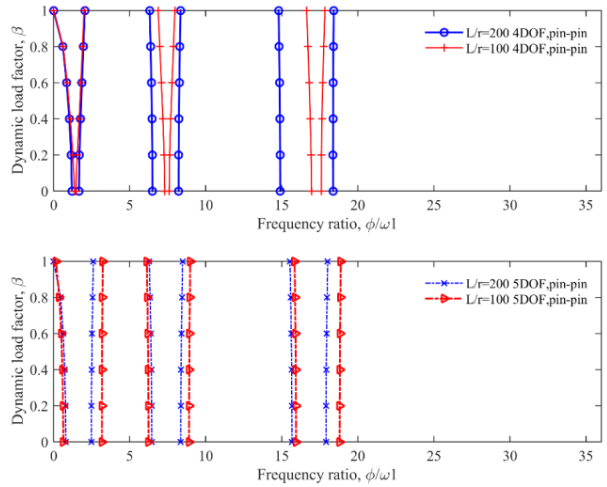


Fig. 7: The Effect of the Slenderness Ratio on the Parametric Instability of Shaft at 0 RPM.

3.3. The effect of the torsional motion

This section is to clarify the effect of the torsional dof that is associated in the 5DOF model on the instability behaviour of the shaft. Figure 8–9 show the percentage difference of the frequency ratios correspond to several points of dynamic load factors β between those of the 4DOF and 5DOF models for the two values of the slenderness ratio studied here. At static condition, the difference in the frequency ratios is zero for both cases of slenderness ratios. At 9000 RPM, the difference between the frequency ratios of the 4DOF and 5DOF models is significant for low slenderness ratio (L/r = 100) that the maximum difference of 21.3% occurs for dynamic load factor of 0. The difference in frequency ratio increases as the rotating speed increases where at 40000 RPM, the difference reaches 117.4 % for the same case of low slenderness ratio. This study shows that especially for shaft with smaller slenderness ratio, the effect of torsional motion that is associated in the 5DOF model is very significant and need to be considered in the design of high speed shaft.

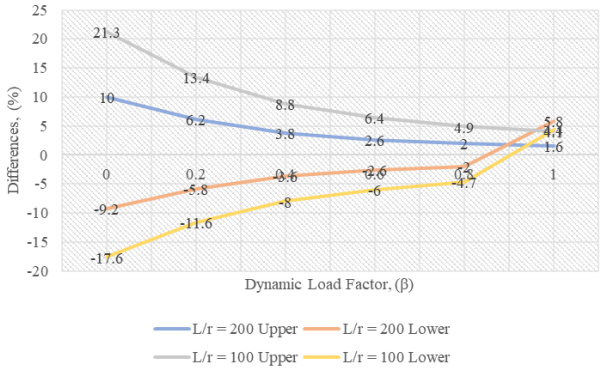


Fig. 8: The Comparison of the First Instability Region between Those of the 4DOF and 5DOF Model at 9000 RPM for Different Slenderness Ratio.

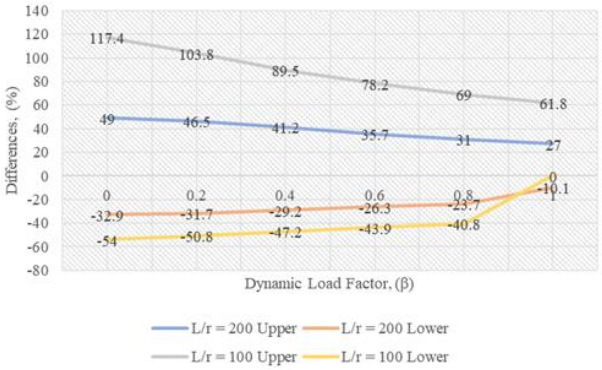


Fig. 9: The Comparison of the First Instability Region between Those of the 4DOF and 5DOF Model at 40000 RPM for Different Slenderness Ratio.

4. Conclusion

A parametric instability analysis was conducted on simple shaft where the effect of the slenderness ratio of the shaft was the focus of the study. The study covered high speed shaft and the effect of torsional motion was included in the formulation. It was found that at static condition, the effect of the slenderness ratio only can be seen at the 3rd mode of instability region. By increasing the speed the shaft, the lower slenderness ratio gives more stability to the shaft especially for higher mode of instability. Furthermore at static condition, the difference in the frequency ratio corresponds to the 4DOF and 5DOF is zero for both cases of high and low slenderness ratios. As the rotating speed increases, the difference in the frequency ratios corresponds to the 4DOF and 5DOF is significant especially for the case of low slenderness ratio of shaft. This proves that the torsional effect of the shaft that is associated to the 5DOF model is significant at higher speed.

Acknowledgement

The authors acknowledge the support in this study from Malaysia-Japan Institute of Technology and Universiti Teknologi Malaysia through the provision of the GUP Grant of Q.K130000.2643. 14J90.

References

[1] Mohanty SC (2007) Parametric Instability of a Pretwisted Cantilever Beam with Localised Damage *Journal of Acoustics and Vibration* 12(4) 1 – 10.

[2] Han Q & Chu F (2012) the effect of transverse crack upon parametric instability of a rotor-bearing system with an asymmetric disk *Communication Nonlinear Science Numerical Simulation* 175189 – 5200. https://doi.org/10.1016/j.cnsns.2012.03.037.

[3] Srinath R. Sarkar A. and Sekhar A.S. (2016) Instability of asymmetric shaft system *Journal of Sound and Vibration* 362 276–291. https://doi.org/10.1016/j.jsv.2015.10.008.

[4] Dakel MZ Baguet S and Dufour R (2014) Steady state dynamic behavior of an on-board rotor under combined base motions *Journal of Vibration and Control* 20 (15) 2254-2287. https://doi.org/10.1177/1077546313483791.

[5] Huang YQ, Lu HW, Fu JY & Liu AR (2014) Dynamic Stability of Euler Beams Under Axial Unsteady Wind Force *Math. Probl. Eng.* 2014 2014 1–12.

[6] Sheu G.J & Yang SM (2005) Dynamic analysis of a spinning Rayleigh beam. *International Journal on Mechanical Science* 47 157–169. https://doi.org/10.1016/j.ijmecsci.2005.01.007.

[7] Liu Z, Ma S, Cai L and Guo T. (2012) Timoshenko Beam-Based Stability and Natural Frequency Analysis for Heavy Load Mechanical Spindles. *Journal of Mechanical Science. Technology* 26 3375–3388.

[8] Bazehhour BG, Mousavi SM & Farshidianfar A (2014) Free Vibration of High-Speed Rotating Timoshenko Shaft with Various Boundary Conditions: Effect Of Centrifugally Induced Axial Force. Archieve in Applied Mechanic 84 1691–1700. https://doi.org/10.1007/s00419-013-0762-5.

[9] Crescimbini F, Lidozzi A, Lo Calzo G & Solero (2014) High-speed electric drive for exhaust gas energy recovery applications *Industrial Electron IEEE Transaction* 61, 2998–3011.

[10] Zorzi ES & Nelson HD (1980) the Dynamics of Rotor-Bearing Systems with Axial Torque—A Finite Element Approach *Journal of Mechanical Design* 102 158. https://doi.org/10.1115/1.3254707.

[11] Nelson HD (1980) A Finite rotating shaft element using timoshenko beam theory *Journal of Mechanical Design* 102 793. https://doi.org/10.1115/1.3254824.

[12] Nelson HD & Mcvaugh JM (1976) the dynamics of rotor-bearing systems using finite elements *Journal of Manufacturing Science and Engineering* 98 593–600. https://doi.org/10.1115/1.3438942.

[13] Bolotin VV (1965) the dynamic stability of elastic systems *American Journal of Physics* 33 752. https://doi.org/10.1119/1.1972245.

[14] Chen LW & Ku DM (1990) Dynamic stability analysis of a rotating shaft by the finite element method *Journal of Sound and Vibration* 143 143–151. https://doi.org/10.1016/0022-460X(90)90573-I.

[15] Sabuncu M. & Evran K. (2005) Dynamic stability of a rotating asymmetric cross-section Timoshenko's beam subjected to an axial periodic force *Finite Element Analysis and Design* 41 1011–1026. https://doi.org/10.1016/j.finel.2004.12.004.